Battery-Aware Contact Plan Design for LEO Satellite Constellations: The Ulloriaq Case Study

Juan A. Fraire, Gilles Nies, Carsten Gerstacker, Holger Hermanns, Kristian Bay, and Morten Bisgaard

***Abstract*—Power demands of communication technologies between LEO small-satellites are difficult to counterbalance by solar infeed and on-board battery storage, due to size and weight limitations. This makes the problem of battery-powered inter-satellite communication a very difficult one. Its management requires a profound understanding as well as techniques for a proper extrapolation of the electric power budget as part of the inter-satellite and satellite-to-ground communication design. We discuss how the construction of contact plans in delay tolerant networking can profit from a sophisticated model of the on-board battery behavior. This model accounts for both nonlinearities in battery behavior as well as stochastic fluctuations in charge, so as to control the risk of battery depletion. We take an hypothetical Ulloriaq constellation based on the GOMX–4 satellites from GomSpace as a reference for our studies.**

***Index Terms*—Satellite constellations, Ad hoc networks, energy management.**

I. INTRODUCTION

THERE is an increasing interest of the space community in deploying large-scale Low-Earth Orbit (LEO) networks with the purpose of providing timely access to information [1]. In-orbit satellites such as the GOMX–4A and GOMX–4B satellites from GomSpace are already pushing for new space-terrestrial communication techniques and technologies capable of efficiently moving data between space and ground networks. Indeed, real-time access to data is only feasible when a chain of links between ground and (potentially several) satellites align to reach a remote destination. As illustrated in Figure 1 a), the lowest datarate on the chain, typically inter-satellite links, becomes the throughput bottleneck. Consequently, communication resources tend to remain largely underutilized.

Manuscript received January 22, 2019; revised May 6, 2019 and August 8, 2019; accepted October 15, 2019. Date of publication November 19, 2019; date of current version March 18, 2020. This work was supported in part by the European Research Council (ERC) Advanced under Grant 695614 (POWVER), and in part by the Deutsche Forschungsgemeinschaft (DFG) under Grant 389792660, as part of TRR 248 (https://perspicuous-computing.science). The associate editor coordinating the review of this article and approving it for publication was E. Ayanoglu. *(Corresponding author: Juan A. Fraire.)*

J. A. Fraire is with the CONICET, Universidad Nacional de Córdoba, Córdoba 5000, Argentina, and also with the Saarland University, Saarland Informatics Campus, 66123 Saarbrücken, Germany (e-mail: juanfraire@gmail.com).

G. Nies and C. Gerstacker are with the Saarland University, Saarland Informatics Campus, 66123 Saarbrücken, Germany.

H. Hermanns is with the Saarland University, Saarland Informatics Campus, 66123 Saarbrücken, Germany, and also with the Software Engineering Research Center, Institute of Intelligent Software, Guangzhou 523898, China.

K. Bay and M. Bisgaard are with GomSpace A/S, 9220 Aalborg, Denmark.

Digital Object Identifier 10.1109/TGCN.2019.2954166

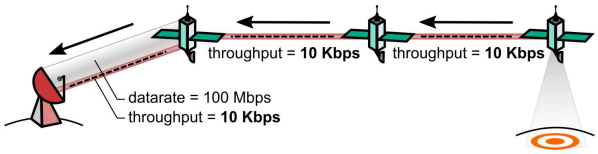

Fig. 1. Low datarate inter-satellite links become the throughput bottleneck of real-time traffic. In a), the space-to-ground link, typically faster because resources, such as large antennas on the ground, are only utilized 0.01%. In b), satellites deliver data to a downlink node in advance to fully use the downlink capacity.

In this context, Delay Tolerant Networking (DTN) has been identified as a disruptive approach which allows for a better utilization of communication opportunities by means of storing, carrying and forwarding data [2]. Store, carry and forward enables a full utilization of available data rate and allows non-latency-constrained data to flow even when the destination is not directly reachable. Therefore, satellites in orbit can prepare data in advance via longer but slower communication opportunities, making an efficient use of shorter but faster downlink opportunities with ground. This is illustrated in Figure 1 b). However, it is crucial to have detailed knowledge on how much power is drained for satellite-to-ground and inter-satellite links, especially when in eclipse, where on-board batteries possibly end up in critically low states of charge. DTN is a perfect fit for this problem as on-board communication subsystems can be scheduled to meet local power resources. Specifically, each satellite's transponder's duty cycle can be embedded into a mutual contact plan, which is computed and designed in advance to provide optimal data delivery throughput and latency.

The contact plan design problem as a means to account for resource-constrained satellites was initially introduced by one of the authors in [3]. Since then, it has received increasing attention from the community. Topological information was first used to assign contacts based on single-hop link assignation fairness metrics in [4], [5]. This work was later extended to also consider multi-hop routing decisions in [6], [7], as well as scheduled and time-varying traffic information thereby further increasing the contact plan design accuracy [8]–[12]. Further efforts in the area also include information on the required satellite mission into the design loop, such as applications for Global Navigation Satellite System (GNSS) [13]. Indeed, the contact plan design problem has proved to be of notable importance for GNSS as a means to optimize the distribution of navigation information between satellites as

shown in [14]–[18]. Also, specific contact plan design tools implementing many of the mentioned contributions have been published and made available in [19], [20].

Works in [21], [22] have recently proposed a linear approximation to energy consumption constraints in the contact plan decision process. However, accurate power budget modeling requires a profound understanding and correct extrapolation of the battery behaviour, which is known to be non-linear. In this sense, authors had addressed the battery-aware task scheduling problem for LEO satellites using detailed battery models [23], [24], but the proposed approach assumed a single (non-networked) satellite. Indeed, the impact on the battery charge of inter-satellite transponders used for in-orbit networking has far been disregarded. To tackle this constellation-wide problem, we propose a Mixed Integer Linear Programming (MILP) model comprising store and forward network flow and linear battery abstractions from which battery-aware communication schedules can be derived. The model is validated with realistic battery models in a possible configuration of the Ulloriaq constellation, based on the GOMX–4A and GOMX–4B satellites.

This paper is structured as follows. An overview of the Ulloriaq case study, the battery model and the battery-aware scheduling procedure are given in Section II. In particular, relevant energy storage models are investigated in Section II-B. Results are analyzed and discussed in Section III. Conclusions are finally summarized in Section IV.

II. System Model

A. Ulloriaq Constellation Overview

GOMX–4A and 4B, launched on February 2017, are 6U CubeSat from GomSpace, commissioned by the Danish Ministry of Defense and the European Space Agency. The overall mission focuses on demonstrating miniaturized technologies, namely orbit maintenance, inter-satellite links, high speed downlink and advanced sensing. These are considered key building blocks for a controlled deployment, operation and maintenance of a future CubeSat-based constellation known as Ulloriaq (the Greenlandic word for "star"). The potential Ulloriaq mission could be aimed at collecting observation and remote sensing data over the Greenland territory to deliver it to a ground station located in Aalborg, Denmark. The proposed space segment is composed of 10 satellites equally separated in the same orbital plane flying in an along-track formation, also known as train formation. As illustrated in Figure 2, the constellation aims at forming a ring around the Earth with a high revisit rate over Greenland territory. As in GOMX–4 mission, satellites are provisioned with two inter-satellite antennas pointing to the front and back neighbor, which allows to timely and cooperatively relay sensed data to the Aalborg ground station.

Table I specifies the ground, orbital and datarate parameters assumed for the Ulloriaq constellation in this study. The latitude and longitude given for the Greenland territory correspond to the centroid of a target area composed of 12750 boundary points that mimic the sensing area. The listed orbital parameters describe a heliosynchronous orbit for each of the 10 satellites, a desired property that guarantees periodic sunlight exposure and eclipse episodes for the constellation. It is also assumed that only two satellites (Sat1 and Sat6) are equipped with a high speed downlink (HSL) transponder. In order to reach the ground station in Aalborg, Denmark via high-speed-link, the data may need to be relayed between satellites via inter-satellite links. However, to properly decide how and when links should be used, battery utilization must be considered.

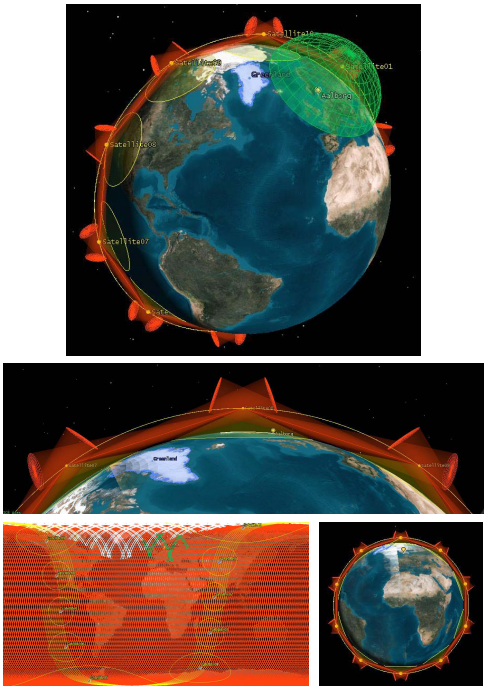

Fig. 2. The proposed configuration for the Ulloriaq constellation. Yellow dots are the satellites, the red cones represents the inter-satellite link antennas visibility.

TABLE I
ULLORIAQ CONSTELLATION PARAMETERS

Ground Segment				
Id		Lat. [deg]	Lon. [deg]	Notes
G	Greenland	73.25	-42.53	Area has 12750 points
A	Aalborg	57.05	9.93	38.53 m of altitude

Space Segment						
Id	Name	Inc. [deg]	RAAN [deg]	T. Anom. [deg]	Avg. Height [km]	Notes
1	Sat1	97.56	168.87	0	540	HSL
2	Sat2	97.56	168.87	36	540	
3	Sat3	97.56	168.87	72	540	
4	Sat4	97.56	168.87	108	540	
5	Sat5	97.56	168.87	144	540	
6	Sat6	97.56	168.87	180	540	HSL
7	Sat7	97.56	168.87	216	540	
8	Sat8	97.56	168.87	252	540	
9	Sat9	97.56	168.87	288	540	
10	Sat10	97.56	168.87	324	540	

Greenland to Sat	Sat to Sat	Sat to Aalborg
10 kbps	10 kbps	100 Mbps (HSL)

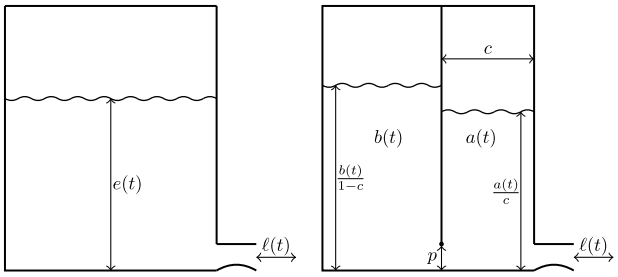

Fig. 3. The one-well representation of the linear battery model (left) and the two-wells representation of the kinetic battery model (right).

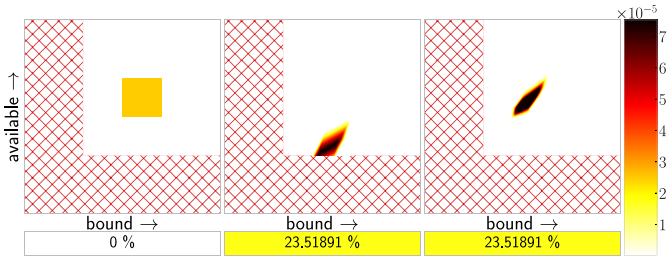

Fig. 4. **Left:** An exemplary KiBaM SoC distribution ($c = 0.5$, $p = 0.05$, $c_{\max} = 200$, $c_{\min} = 30$) with an uniformly distributed initial SoC over the area [50, 70] × [50, 70]. The unsafe region (below $c_{\min}$) is represented as red hatched areas. **Middle:** After discharging for 6 time units with a noisy load of 5.5 whose noise model is a truncated Gaussian with support $[-1, 1]$. Roughly 23.5% of the probability mass depletes (indicated at the bottom of the graph) and is accumulated in the bottom part, where it remains. **Right:** After charging the remaining 74.5% for 3 time units with a load of -7.

B. Linear Battery Model vs. Kinetic Battery Model

In order to reason about energy consumption we need a faithful formal representation of energy storage in satellites. In the majority of cases Li-ion battery packs are used in CubeSat missions. Ulloriaq will be no exception. We introduce two battery models that are often used in that context and considered in this work. A thorough comparison of state-of-the-art formal battery models can be found in [25].

1) Linear Battery Model: The *Linear Battery Model* (LiBaM) is arguably the most used and simple model of energy storage. It is often thought of as a well holding fluid that can be drained or refilled as seen in Figure 3. Let $\ell(t)$ be a piecewise constant function, representing the *load* on the battery. Then, the battery's state of charge $e(t)$ evolves piecewise linearly over time t and proportionally to $\ell(t)$, i.e., $\dot{e}(t) = \ell(t)$, where $\dot{e}$ is the time derivative of e. The load represents charging and discharging if $\ell(t) < 0$ and $\ell(t) > 0$, respectively. We consider the battery to be critical if $e(t) \leq c_{\min}$, where $c_{\min} \geq 0$ is referred to as the *safe* threshold. The model can be extended easily by a capacity limit $c_{\max}$: If $e(t)$ hits $c_{\max}$ during a charging period, it simply remains at $c_{\max}$ for the remainder of that period. Batteries are however inherently nonlinear, thus the LiBaM is an unjustifiably optimistic model of energy storage.

2) Kinetic Battery Model (KiBaM): The *Kinetic Battery Model* (KiBaM) improves over the LiBaM by splitting the stored charge into two portions, namely (i) the available charge $a(t)$, that is directly affected by the load on the battery, and (ii) the bound charge $b(t)$, that is not directly influenced by the load, but is rather chemically bound inside the battery.

Bound charge is converted into available charge over time (or vice-versa) via diffusion from one well to the other. The diffusion speed is regulated by the non-negative parameter p and is proportional to the difference in height of both wells, while $c \in [0, 1]$ specifies the fraction of available charge. The KiBaM is often depicted as two interconnected wells holding fluid (see Figure 3). Mathematically, the KiBaM follows two coupled differential equations: $\dot{a}(t) = -\ell(t) + p \cdot (b(t)/(1-c) - a(t)/c)$ and $\dot{b}(t) = p \cdot (a(t)/c - b(t)/1-c)$. The dynamics of the KiBaM account for a couple of nonlinear effects that can be observed on real-world batteries, like the *recovery effect* and the *rate-capacity effect*, both rooted in the relatively slow conversion of bound charge into available charge. The battery is assumed to be at a critically low charge level if the available charge drops to or below a safety threshold $c_{\min}$, i.e., if $a(t) \leq c_{\min}$. Notably, even for $c_{\min} = 0$ some energy will be left in the battery in chemically bound form on hitting the threshold. The KiBaM has been extended by capacity limits as well as stochastic fluctuations in charge and loads [26] in order to get tight bounds on battery depletion risks in cases when the initial state of charge might be uncertain. For the work presented here it suffices to introduce the visualization of these so called State of Charge (SoC) distributions along a sequence of load distributions. For a detailed and rigorous treatment of this *stochastic* KiBaM we refer to [26].

A SoC distribution is visualized as two stacked plots, (i) the top part being a heatmap representing the probability density function of the two-dimensional KiBaM SoC on the range from depletion to the battery capacity limits, with the available and bound charge on the y-axis and x-axis respectively, and (ii) the bottom part being the accumulated depletion risk as a color coded probability value. Figure 4 depicts the evolution of an example SoC distribution along an example load sequence.

In the context of satellites constellations, the state of charge of on-board batteries conditions the selection on wether an ISL or ground-to-satellite link can be established or not, in a given time interval. To this end, in the following section, we propose a model that leverages the discussed battery models to support a battery-aware scheduling of the space network.

C. Mixed-Integer Linear Programming Model

In order to tackle the battery-aware link scheduling problem for DTN satellite networks, we consider an abstraction of the satellite constellation based on a discrete set of time episodes where the topology is considered stable and can be modeled by a temporary static graph. As thoroughly discussed in [9], a set of K states, each of them comprised of a static graph with N nodes valid during a specific period of time $(t_k; t_{k+1})$, can be used to represent the time-evolving network connectivity. Figure 5 a) illustrates four successive states where the connectivity of the constellations evolves as follows: from k_1 to k_2, the ground station A stops seeing satellite 3 and sees satellite 2; from k_2 to k_3, the observation target is no longer

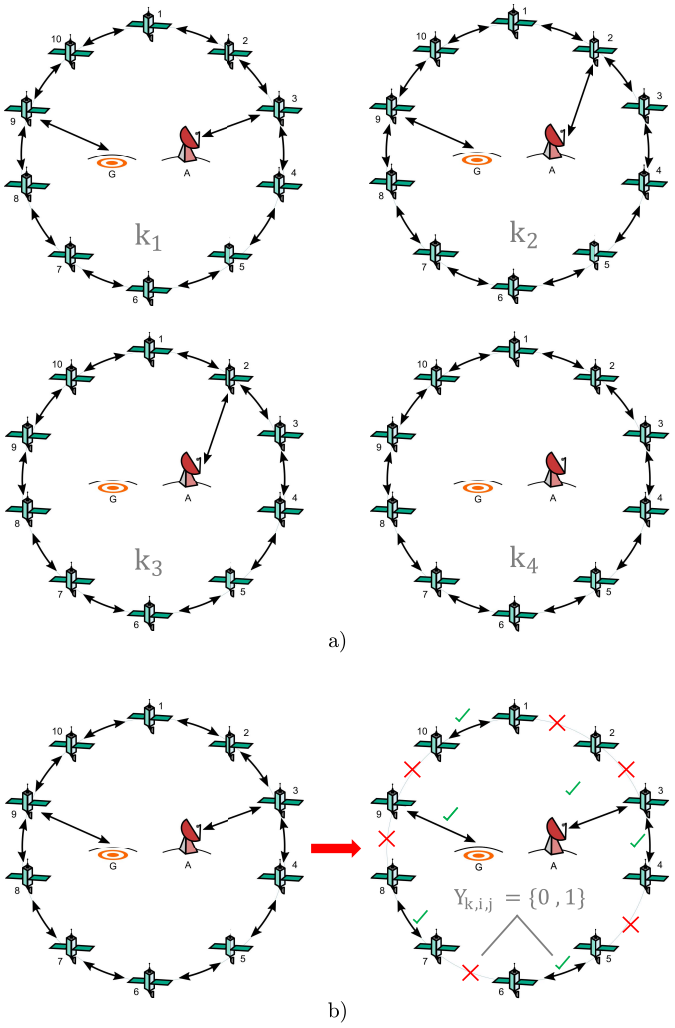

Fig. 5. Time-evolving topology model based on discrete time episodes in a). This model facilitates the scheduling on contacts on each of this episodes as shown in b).

visible by satellite 9; from k_3 to k_4 the ground station looses the link with satellite 2. In other words, whenever a communication opportunity starts or ends, a new state is added to the topology to describe the new connectivity. However, in a battery-aware model, a state change is also triggered by a change from sunlight exposure to eclipse, since it represents a transition from charging to discharging (and vice-versa) of the on-board batteries. This formulation for time-evolving predictable networks enables to choose on a per-state basis which contacts are enabled and which are to be disabled. As illustrated in Figure 5 b), procedures can be defined to schedule the utilization of resources in advance based on the expected traffic, topology and the available satellite resources.

Auxiliary coefficients such as contact capacity ($\{c_{k,i,j}\}$), buffer capacity ($\{b_i\}$) and traffic sources ($\{d_k^{i,j}\}$) can be used to complete the abstraction of the satellite constellation. Battery coefficients are included as part of the model and specified by the minimum and maximum battery charge allowed ($\{c_{\min,i}\}$ and $\{c_{\max,i}\}$) as well as the initial charge

TABLE II
MILP MODEL PARAMETERS

Input Coefficients	
N	Nodes quantity
K	Topology states quantity
$\{t_k\}$	State k start time ($1 \leq k \leq K$)
$\{i_k\}$	State k duration ($i_k = t_k - t_{k-1}$: $1 \leq k \leq K$)
$\{x_{k,i,j}\}$	Capacity of i to j contact at state k ($1 \leq k \leq K$ and $1 \leq i, j \leq N$)
$\{b_{\max,i}\}$	Maximum buffer capacity at node i ($1 \leq i \leq N$)
$\{d_k^{i,j}\}$	Traffic from i to j originated at the beginning of k ($1 \leq k \leq K$ and $1 \leq i, j \leq N$)
$\{p_i\}$	Max. simultaneous links in node i ($1 \leq i \leq N$)
M	Big "M" coefficient for interface decision equations
$\{c_{\min,i}\}$ $\{c_{\max,i}\}$	Minimum and maximum battery charge at node i ($1 \leq i \leq N$) at all times
$\{c_{0,i}\}$	Initial battery charge at node i
$\{c_{rC}^i\}$	Battery recharge rate because of sunlight exposure at node i, if on eclipse, then this coefficient shall be 0
$\{c_{rT}^i\}$	Battery consumption rate because of transmission or reception system enabled at node i
$\{c_{rB}^i\}$	Battery consumption rate because of background load at node i

Output Variables	
$\{X_{k,i,j}^{y,z}\}$	Traffic from y to z at state k flowing in i to j edge ($1 \leq i, j, y, z \leq N$)
$\{B_{k,i}^{y,z}\}$	Node i buffer occupancy at the end of state k by the traffic flow from y to z ($1 \leq i, y, z \leq N$)
$\{Y_{k,i,j}\}$	Binary variable for link selection from i to j at state k ($1 \leq k \leq K$ and $1 \leq i, j \leq N$)
$\{C_{k,i}\}$	Battery charge at node i at the end of state k ($1 \leq k \leq K$ and $1 \leq i, j \leq N$)

($\{c_{0,i}\}$). The battery is recharged only if the spacecraft is currently exposed to sunlight by the difference of the solar infeed ($\{c_{rC}^i\}$) and the link activity (given by $\{c_{rT}^i\}$ and $\{c_{rB}^i\}$). As output variables we designate the traffic flowing through the network ($\{X_{k,i,j}^{y,z}\}$), the buffer occupancy as states evolve ($\{B_{k,i}^{y,z}\}$), link utilization variables ($\{Y_{k,i,j}\}$), and the LiBaM state of charge at the end of each state ($\{C_{k,i}\}$). Model parameters are summarized in Table II.

A Mixed-Integer Linear Programming (MILP) model can be specified based on these coefficients and variables. MILP models are a well-studied variation of classical linear programming (LP) where some of the variables are constrained to be integers or Booleans. In contrast to LP which is known to be of polynomial worst case complexity [27], MILP is known to be NP-hard [28]. Practically efficient solvers, often based on branch-and-bound/branch-and-cut approaches for the integer fragments of the problems are available, such as IBM ILOG CPLEX [29] or Gurobi [30].

In our model, Equations (2) to (6) are the constraints of a time-evolving statement of the known multi-commodity flow problem which has already been applied for store, carry and forward satellite networks in [9]. Specifically, equation (2) models the evolution of data as it either flows between nodes ($\{X_{k,i,j}^{y,z}\}$) or is kept in a local storage ($\{B_{k,i}^{y,z}\}$). Equations (3) and (4) specifies the maximum and initial status of each node's buffer. Equation (5) specifies the maximum flow of data that can be sent over each contact. Equation (6) sets the flow imbalance, or traffic demands ($d_k^{i,j}$) from all

source to destination nodes.

$$\text{minimize:} \sum_{k=1}^{K}\sum_{i=1}^{N}\sum_{j=1}^{N}\sum_{y=1}^{N}\sum_{z=1}^{N} w_t(t_k)\cdot X_{k,i,j}^{y,z} + w_y \cdot Y_{k,i,j} - w_c \cdot C_{k,i} \quad (1)$$

$$\text{Subject to:} \sum_{j=1}^{N} X_{k,j,i}^{y,z} - \sum_{j=1}^{N} X_{k,i,j}^{y,z} = B_{k,i}^{y,z} - \left(B_{k-1,i}^{y,z} + d_k^{i,z}\right) \quad \forall k,i,y,z \quad (2)$$

$$\sum_{y=1}^{N}\sum_{z=1}^{N} B_{k,i}^{y,z} \le b_{\max}^{i} \quad \forall k,i,y,z \quad (3)$$

$$B_{0,i}^{y,z} = 0 \quad \forall i,y,z \quad (4)$$

$$\sum_{y=1}^{N}\sum_{z=1}^{N} X_{k,i,j}^{y,z} \le x_{k,i,j} \quad \forall k,i,j \quad (5)$$

$$\sum_{k=1}^{K}\sum_{i=1}^{N} X_{k,i,z}^{y,z} - \sum_{k=1}^{K}\sum_{j=1}^{N} X_{k,z,j}^{y,z} = \sum_{k=1}^{K} d_k^{y,z} \quad \forall y,z \quad (6)$$

$$\sum_{j=1}^{N} Y_{k,i,j} \le p_i \quad \forall i,k \quad (7)$$

$$\sum_{y=1}^{N}\sum_{z=1}^{N} X_{k,i,j}^{y,z} \le M \cdot Y_{k,i,j} \quad \forall i,k,j \quad (8)$$

$$C_{0,i} = c_{0,1} \quad \forall i \quad (9)$$

$$c_{\min}^{i} \le C_{k,i} \le c_{\max}^{i} \quad \forall k,i \quad (10)$$

$$C_{k,i} \le C_{k-1,i} + \left(c_{rC}^{i} - c_{rB}^{i} - c_{rT}^{i}\sum_{j=1}^{N} Y_{k,i,j}\right) \times t_k \quad \forall k,i \quad (11)$$

The rest of the equations specifies resources limitations to the former flow model. Equations (7) and (8) provide a mechanism to bound the maximum quantity of simultaneous communications a given node can establish at any given moment. In this work, we have set $p_i = 3$ meaning that at most two inter-satellite links and one ground station link can be used. Equation (9) is used to set the initial battery state of charge, Equation (10) bounds the battery charge at all states and Equation (11) models the evolution of charge throughout states using the LiBaM. Given these constraints, the objective function in (1) aims at obtaining an optimal traffic flow assignment (expressed in data volume units such as Bytes), where later flows are penalized by a $w_t(t_k)$ cost function that increases with time. Furthermore, $Y_{k,i,j}$ binary variables are also minimized with weight w_y as a precautionary measure to shut down interfaces whenever constraint in Equation (8) allows for it. $C_{k-1,i}$ battery charge variables (expressed in charge units such as Joules), are minimized with weight w_c to force battery charge to be drained down to the limit of constraints in Equations (10) and (11). As a result, the objective function combines three terms with different units whose respective influence can be balanced by configuring their respective weights. In this work, we set $w_c = 1$, $w_y = 1$ and $w_t(t_k) = t_k$.

As a result, an optimal traffic assignment can be obtained, and a battery-aware contact plan can be provisioned to the constellation to enable the utilization of communication resources while minimizing battery exhaustion probability. Unfortunately, although the MILP model includes the LiBaM formulation, the latter might not accurately reflect the real battery behavior, which is not linear. However, the KiBaM cannot be expressed within the MILP due to its non-linearity. As to be discussed in Section III, safe margins shall thus be considered when using the linear model. As an additional quality assurance and potential refutation mechanism, the contact plan synthesized with the LiBaM included in the MILP can be validated using the vastly more accurate stochastic KiBaM in a post-processing step. This is indeed what we do.

TABLE III
BATTERY MODEL PARAMETERS

	Absolute	Relative
Total battery capacity	277056.0 J	100 %
Initial battery charge	221644.8 J	80 %
Minimal battery charge at all times	166233.0 J	50 + 10 %
Background consumption rate	4.630 J/s	0.001671 %/s
Tx/Rx consumption rate	13.651 J/s	0.004927 %/s
Recharge by sunlight exposure rate	15.472 J/s	0.005584 %/s

III. RESULTS AND ANALYSIS

We set the model based on the Ulloriaq connectivity and feed it with a total of 187.5 MB (1500 Mbit) of data to be transmitted from the Greenland territory at the beginning of a 48 hs analysis window. It is worth noticing that such amount of transferred data is far from saturating the local memory buffers of satellites which are configured to 512 MB, a conservative memory storage given commercially available CubeSat subsystems. The scenarios and the resulting contact plans were generated using the System Tool Kit (STK) and the Contact Plan Designer plug-in [19]. The contact topology comprising all possible communication opportunities is presented in Figure 6 and requires of a model of $k = 1240$ states. The figure indicates inter-satellite communications (in red) could be continuously enabled throughout the 48 hours. This is because neighbouring satellites in the back and the front are always at sight. However, as previously discussed, power budget constraints forbids a continuous utilization of the ISL resources. Figure 7 illustrates the contact plan where only direct, or non-store-carry-and-forward data flow is present between Aalborg and Greenland. In this case, data is not stored but instantaneously transferred from one node to the other. When such an end-to-end exchange is employed, the end-to-end throughput is bounded lowest data rate in the exchange. For the example chain shown in Figure 7, the HSL allows for 100 Mbps, but the lowest data rate in the ISLs (10 kbps) becomes the bottleneck in the transaction. Although any satellite's batteries would hardly deplete on such a low transponder utilization, a DTN approach is appealing to increase the overall data delivery at the price of higher latencies.

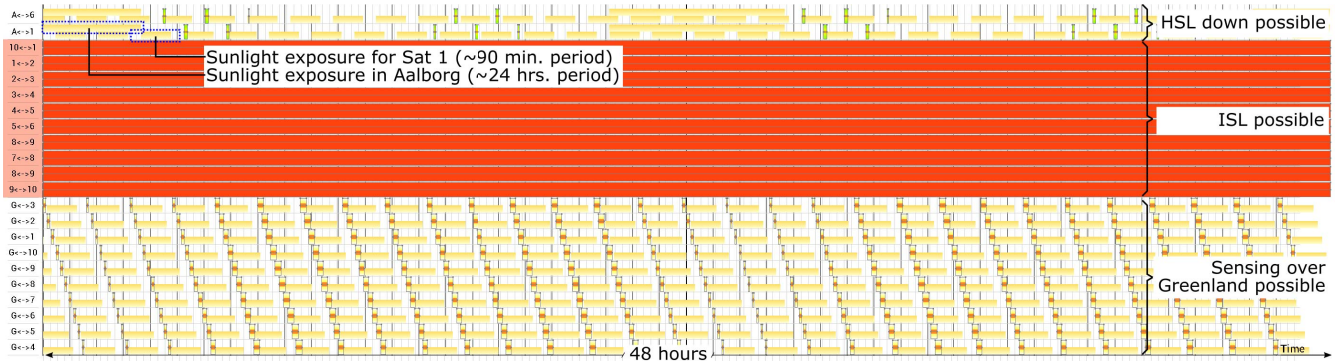

Fig. 6. Ulloriaq topology. The horizontal axis represents the 48 hours timeline, ordinates are node pairs. HSL downlink link possibilities are plotted in green between satellite 1 and 6 to Aalborg ground station (A). Inter-satellite links (in red) can be permanently enabled as satellites are in continuous range of the front and back neighbors. Several sensing opportunities between Greenland territory (G) and each of the 10 satellites are highlighted as small orange boxes at the bottom. Finally, sunlight exposures for each node are indicated by a yellow background. Sunlight conditions vary with a period of about 90 minutes, which is the orbital period of satellites in LEO.

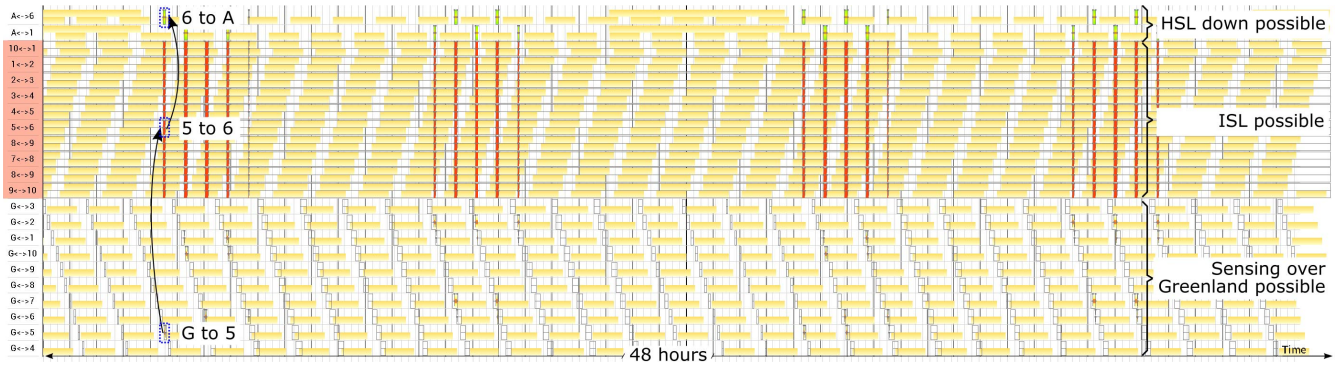

Fig. 7. Contact plan with direct end-to-end paths (i.e., no store-carry-and-forward) between Greenland and Aalborg. Data transfers only happens when a chain of links can be established from Aalborg to Greenland. In the figure, the chain G, 5, 6, A is highlighted, indicating sensed data from Greenland can be directly delivered to Aalborg using one ISL link between satellite 5 and 6.

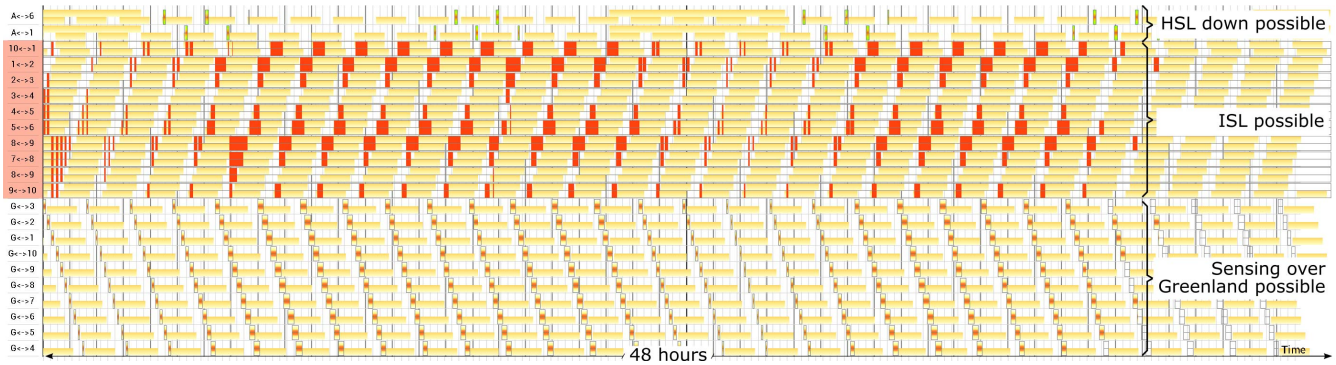

Fig. 8. DTN contact plan without battery awareness. Inter-satellite links resources exhibits a higher utilization than in Figure 7. The increment can be visualized by observing the larger periods of time where ISL possibilities are highlighted in red. This improvement in connectivity among satellites enables a larger amount of collected data to be delivered to Aalborg.

Two possible DTN schedules are studied, one is obtained without restrictions to battery utilization, and another with battery constraints in terms of a simplistic LiBaM, using the MILP model with battery parameters listed on Table III. A 10% safety margin is added to the minimal battery charge at all times in order to account for the idealistic nature of the LiBaM. By using state-of-the-art IBM ILOG CPLEX solver v12.8.0.0 on an Intel i5 processor with 4 GiB of RAM running an Ubuntu 18.04.2 OS, the model is solved in 10 minutes. As reported in [29], IBM CPLEX software solves MILP models using well-known branch and bound algorithms. Branch and bound algorithms exploits a systematic enumeration of candidate solutions (a.k.a state space search) to tackle discrete and combinatorial optimization problems, as well as mathematical optimization [31]. Both resulting schedules are illustrated in Figures 8 and 9 respectively. The schedule with battery awareness forces the network to distribute the utilization of communication resources in space and time resulting

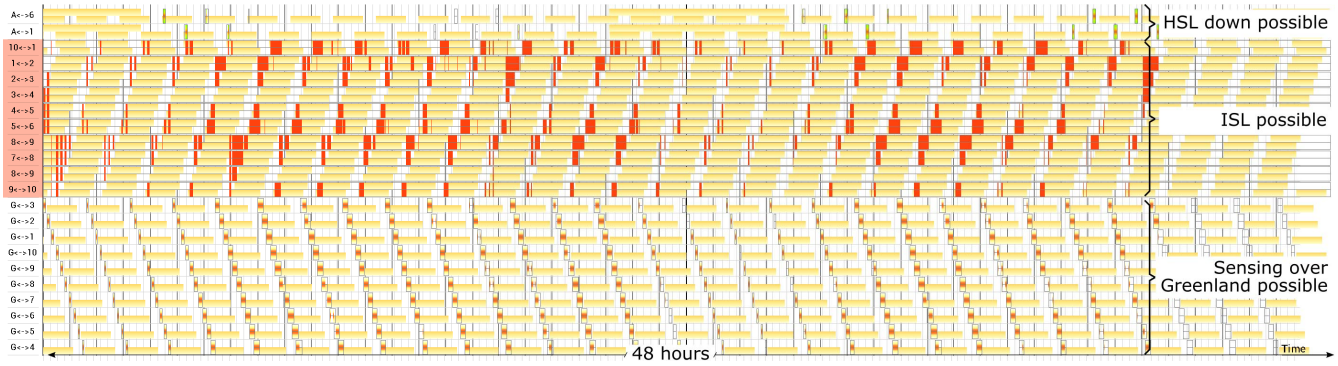

Fig. 9. DTN contact plan with battery awareness.

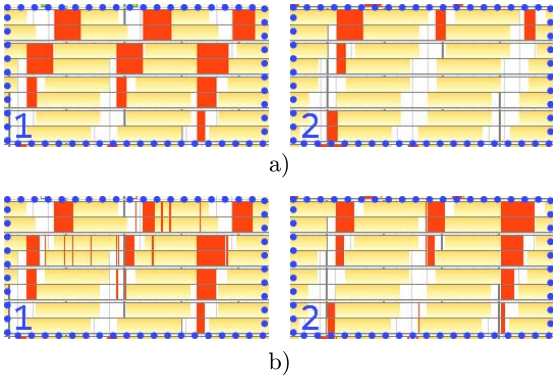

Fig. 10. Detailed view of contact plans obtained from the non-battery aware model (Figure 8) in a) and the battery-aware method (Figure 9) in b). In rectangle 1, the non battery-aware schedule provides a more concentrated utilization of resources during most of the contact plan period. In rectangle 2, the battery-aware contact plan requires the utilization of communication opportunities towards the end of the contact plan in order to compensate the earlier battery-aware contention.

TABLE IV
DATA DELIVERED IN 48 HS

Schedule	Delivered Data
Real-time contact with Greenland (Figure 7)	7.9 MBytes
Battery-agnostic store-carry-and-forward (Figure 8)	187.5 MBytes
Battery-aware store-carry-and-forward (Figure 9)	167.4 MBytes

TABLE V
THE RISK OF DROPPING BELOW A STATE OF CHARGE THRESHOLD OF 50% IN THE BATTERY-AGNOSTIC CONTACT PLAN OF FIGURE 8 AND THE BATTERY-AWARE CONTACT PLAN OF FIGURE 9

Satellite Id	Depletion Risk [%]	
	Battery-agnostic	Battery-aware
1	100	0.16
2	0.17	0
3	0	0
4	0	0
5	0	0
6	100	0.038
7	50.73	0
8	0	0
9	0	0
10	0	0

in a less concentrated contact plan than the battery-agnostic one. This is particularly noticeable in the inter-satellite link assignation (red colored schedule). Figure 10 depicts in higher detail how the battery-aware approach spreads the utilization of communications resources

The total delivered data of each of these link schedules are summarized in Table IV. On the one hand, it is evident from Figure 7 that constraining the communication to a real-time end-to-end type only renders a very low transfer of data volume, 7.9 MB out of 187.5 MB (less than 0.5% of the data available for transmission). On the other hand, a store-carry-and-forward approach enables almost a 100% of data delivery when battery SoC are disregarded, and 89.3% when ISL and ground-to-satellite transmissions are bounded with battery models. Indeed, in the latter, data flow between satellites and between satellites and ground stations can only happen when enough power is available on the satellites. This means that, unlike the battery-aware scheme, the resulting schedule obtained from the battery-agnostic scheme, although better in terms of data delivery, cannot be provisioned to a real satellite network as it comes with a substantial risk of depleting on-board batteries.

To analyze the battery utilization, and in particular the risk of dropping below a certain state of charge threshold,we validated the contact plans with respect to the closer-to-reality stochastic KiBaM with parameters $c = 0.5$ and $p = 0.0005$. The uncertainty model around the initial state of charge $a(0)$, $b(0)$ is truncated Gaussian with a support ranging $[-4\%, 4\%]$ in both the available and the bound charge dimensions. We additionally assume piecewise truncated white noise around the loads with support of $[-0.5, 0.5]$ J/s.

The risk of dropping below a safe battery threshold of 50% for each satellite involved in the battery-agnostic contact plan is summarized in Table V. In a battery-agnostic context we see that half of the satellites drop below a critically low state of charge level with certainty, while the battery-aware contact plan causes the satellites to reach such an undesired area with a probability of around 25% at worst. Most satellites exhibit a negligible risk ($\leq 1\%$) of attaining critically low battery levels.

Figure 11 depicts the state of charge evolution of satellite 5 in the battery-aware as well as the battery-agnostic setting. Each plot consist of two subplots, (i) Several KiBaM evolutions on top, showing the most optimistic and the most

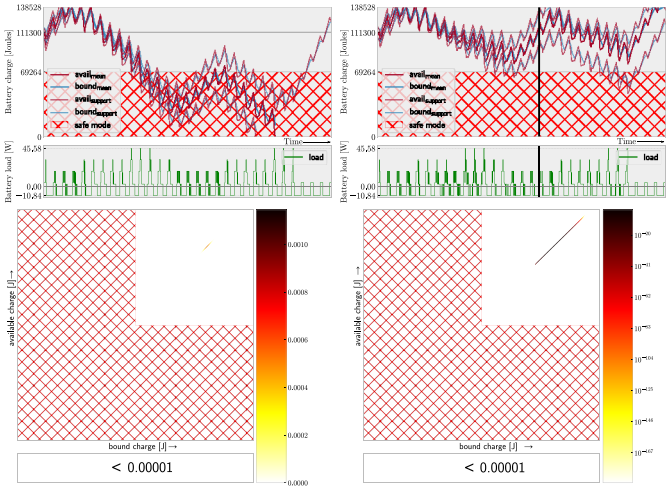

Fig. 11. **Top:** The state of charge evolution of satellite 1 in the battery-agnostic (left) as well as the battery-aware setting (right). The former reveals certain premature battery depletion. The latter induces a slightly more spread out load profile. Even though its worst-case evolution exposes a risk of depletion, the improvement with respect to the battery-agnostic plan is obvious. **Bottom:** The SoC distribution of the quantitative validation of the battery-aware plan at the time point indicated by the black vertical line of the battery-aware plan on a linear (left) as well as on a logarithmic (right) color scale, revealing a negligible accumulated depletion risk. This time point was chosen purposely and suitably to enhance visualisation quality of the SoC distributions.

pessimistic evolution (dashed lines) as well as the mean evolution (solid), and (ii) the load sequence entailed by the contact plan on the bottom. The mean evolution is the KiBaM counterpart to the LiBaM evolution computed in the MILP; with an initial state of charge of $a(0) = 80\%$ and $b(0) = 80\%$, we track its evolution along the load sequence induced by the contact plan. The best case is computed by slightly overapproximating the highest initial state of charge that is supported by the Gaussian uncertainty, i.e., $a(0) = 80{+}4\%$ and $b(0) = 80{+}4\%$ and tracking it along the sequence of best-case loads among those that have support in the load noise model, i.e., $\ell(t) - 0.5$ J/s in every step. The worst case is symmetric to the best case by picking $a(0) = 80{-}4\%$ and $b(0) = 80{-}4\%$ and $\ell(t) + 0.5$ J/s. Thus, the dashed lines span the corridor of reachable (with positive probability) states of charge along time. Consequently, if the corridor never intersects with the region of undesirably low SoCs (red hatched area), depletion is impossible. Similarly, if even the best-case evolution drops below that threshold, the satellite surely depletes. The borderline, and most interesting case is if the worst-case evolution drops below the threshold but the best-case does not. In this case, we need to quantify the depletion risk by tracking the whole state of charge distribution over time, as explained at the end of Section II-B.

A. Discussion

1) Discretization: The MILP model captures the time evolution of the topology in K discrete time intervals and decisions on resources utilization are thus limited to such intervals. However, the fact that Ulloriaq satellites stay in reach of each other continuously render a time-continuous scheduling possible. Moving to a finer-grain discretization, by slitting long intervals into smaller ones, can improve the scheduling at the expense of higher processing effort in solving a larger and more complex model. Exploring optimal discretization of intervals or alternative time-continuous strategies is an appealing future research area in the battery-aware planning.

2) Model Accuracy: We analyzed the generated contact plan with the more realistic stochastic KiBaM model as an a-posteriori validation. Indeed, contact plans complying with a linear battery model might need to be rejected in case of non-negligible depletion risk determined by more accurate models. In our case study, a safety-margin of 10% turned out to deliver satisfactory results. Nonetheless, to successfully tackle general cases, a heuristic approach that iteratively finds optimal margins for each scenario seems worthwhile to be considered for future battery-aware contact planning.

3) Real-Time Traffic: Store-carry-and-forward was studied as a more flexible approach that allows to conveniently decide on transponder duty cycle and thus on battery utilization. However, in the future Ulloriaq mission, real-time traffic would need to be also considered in the model and treated with priority when a direct connection to Greenland is possible from Aalborg. The remaining capacity can then be used for higher latency data. Although including traffic priorities is possible in state-of-the-art DTN protocols, properly modeling this phenomenon in the proposed MILP model is left as a continuation and extension of this work.

4) Other Means of Contact Plan Synthesis: Other methods of temporal planning and constraint solving could be used to synthesize battery-aware contact plans. The formalism of *Timed Automata* or its *Priced* extension have been applied numerous times to a variety of scheduling problems. The recently emerging field of *Optimization Modulo Theories* (OMT), an extension of the well-known *Satisfiability Modulo Theories* (SMT) problem, provides a similar formulation of contact plan synthesis than MILP. Several (potentially conflicting) objective functions can be optimized with descending priority in order to account for multiple goals.

IV. Conclusion

The power budget of small-satellites such as GomX–4A and B are very demanding when considered for networked constellations. A permanent communication link is not to be sustainable only for bounded periods. As a result, we have investigated the utilization of store-carry-and-forward approach to optimize data delivery and battery utilization.

By means of a MILP model, optimal contact plans in terms of data delivery volume and time were determined. By including linear battery constraints, the designed contact plans also allowed to minimize the probability of battery exhaustion in power-constrained satellites. We found that a 10% safe-margin was enough to meet the battery charge conditions as calculated by realistic state-of-the-art battery models.

Future work could be focused on improving model accuracy by leveraging non-linear modeling to include KiBaM equations. However, leaving the linear approach immediately

makes things either undecidable or completely inefficient, limiting the applicability of the solution. On the contrary, the most appealing research line is the extension of the proposed two-step procedure (LiBaM validated by KiBaM) to derive compute-efficient schemes in bounded time. Indeed, the resulting information need to be timely provisioned to the satellite network as satellites passes over the ground station.

Demonstrated by the results of a first realistic case study inspired in a potential Ulloriaq constellation, the battery-aware contact plan design is envisioned as a valuable scheduling procedure to make an optimal use of resources in future networked small-satellite constellations.

ACKNOWLEDGMENT

Part of this work has been developed while Dr. J. Fraire was visiting Politecnico di Torino.

REFERENCES

[1] J. Alvarez and B. Walls, "Constellations, clusters, and communication technology: Expanding small satellite access to space," in *Proc. IEEE Aerospace Conf.*, Big Sky, MT, USA, Mar. 2016, pp. 1–11.

[2] V. Cerf *et al.*, "Delay-tolerant networking architecture," IETF, RFC 4838, Apr. 2007. [Online]. Available: http://www.rfc-editor.org/rfc/rfc4838.txt

[3] J. A. Fraire and J. M. Finochietto, "Design challenges in contact plans for disruption-tolerant satellite networks," *IEEE Commun. Mag.*, vol. 53, no. 5, pp. 163–169, May 2015.

[4] J. A. Fraire, P. Madoery, and J. M. Finochietto, "On the design of fair contact plans in predictable delay-tolerant networks," in *Proc. IEEE Int. Conf. Wireless Space Extreme Environ. (WiSEE)*, Baltimore, MD, USA, Nov. 2013, pp. 1–7.

[5] J. A. Fraire, P. G. Madoery, and J. M. Finochietto, "On the design and analysis of fair contact plans in predictable delay-tolerant networks," *IEEE Sensors J.*, vol. 14, no. 11, pp. 3874–3882, Nov. 2014.

[6] J. A. Fraire and J. M. Finochietto, "Routing-aware fair contact plan design for predictable delay tolerant networks," *Ad Hoc Netw.*, vol. 25, pp. 303–313, Feb. 2015.

[7] C.-Q. Dai and H. Tang, "Genetically inspired contact plan design in small satellite networks," in *Proc. Int. Conf. Comput. Inf. Telecommun. Syst. (CITS)*, Dalian, China, Jul. 2017, pp. 113–117.

[8] J. A. Fraire, P. G. Madoery, J. M. Finochietto, and G. Leguizamón, "Preliminary results of an evolutionary approach towards contact plan design for satellite DTNs," in *Proc. IEEE Int. Conf. Wireless Space Extreme Environ. (WiSEE)*, Orlando, FL, USA, Dec. 2015, pp. 1–7.

[9] J. A. Fraire, P. G. Madoery, and J. M. Finochietto, "Traffic-aware contact plan design for disruption-tolerant space sensor networks," *Ad Hoc Netw.*, vol. 47, pp. 41–52, Sep. 2016.

[10] J. A. Fraire, P. G. Madoery, J. M. Finochietto, and G. Leguizamón, "An evolutionary approach towards contact plan design for disruption-tolerant satellite networks," *Appl. Soft Comput.*, vol. 52, pp. 446–456, Mar. 2017.

[11] Y. Wang, M. Sheng, J. Li, X. Wang, R. Liu, and D. Zhou, "Dynamic contact plan design in broadband satellite networks with varying contact capacity," *IEEE Commun. Lett.*, vol. 20, no. 12, pp. 2410–2413, Dec. 2016.

[12] D. Zhou, M. Sheng, J. Li, C. Xu, R. Liu, and Y. Wang, "Toward high throughput contact plan design in resource-limited small satellite networks," in *Proc. IEEE 27th Annu. Int. Symp. Pers. Indoor Mobile Radio Commun. (PIMRC)*, Valencia, Spain, Sep. 2016, pp. 1–6.

[13] H. Yan, Q. Zhang, and Y. Sun, "Local information-based congestion control scheme for space delay/disruption tolerant networks," *Wireless Netw.*, vol. 21, no. 6, pp. 2087–2099, 2015, doi: 10.1007/s11276-015-0911-6.

[14] X. Chu and Y. Chen, "Time division inter-satellite link topology generation problem: Modeling and solution," *Int. J. Satellite Commun. Netw.*, vol. 36, no. 2, pp. 194–206, 2017.

[15] J. Huang, W. Liu, Y. Su, and F. Wang, "Cascade optimization design of inter-satellite link enhanced with adaptability in future GNSS satellite networks," *GPS Solutions*, vol. 22, no. 2, p. 44, Apr. 2018.

[16] J. Huang, Y. Su, W. Liu, and F. Wang, "Optimization design of inter-satellite link (ISL) assignment parameters in GNSS based on genetic algorithm," *Adv. Space Res.*, vol. 60, no. 12, pp. 2574–2580, 2017.

[17] D. Yang, J. Yang, and P. Xu, "Timeslot scheduling of inter-satellite links based on a system of a narrow beam with time division," *GPS Solutions*, vol. 21, no. 3, pp. 999–1011, Jul. 2017.

[18] L. Sun, Y. Wang, W. Huang, J. Yang, Y. Zhou, and D. Yang, "Inter-satellite communication and ranging link assignment for navigation satellite systems," *GPS Solutions*, vol. 22, no. 2, p. 38, Apr. 2018.

[19] J. A. Fraire, "Introducing contact plan designer: A planning tool for DTN-based space-terrestrial networks," in *Proc. 6th Int. Conf. Space Mission Challenges Inf. Technol. (SMC-IT), STINT-DEMO Workshop*, Alcala de Henares, Spain, Sep. 2017. [Online]. Available: https://doi.org/10.1109/SMC-IT.2017.28

[20] J. A. Fraire, P. Madoery, F. Raverta, J. M. Finochietto, and R. Velazco, "DtnSim: Bridging the gap between simulation and implementation of space-terrestrial DTNs," in *Proc. 6th Int. Conf. Space Mission Challenges Inf. Technol. (SMC-IT), STINT-DEMO Workshop*, Alcala de Henares, Spain, Sep. 2017, pp. 120–123.

[21] D. Zhou, M. Sheng, X. Wang, C. Xu, R. Liu, and J. Li, "Mission aware contact plan design in resource-limited small satellite networks," *IEEE Trans. Commun.*, vol. 65, no. 6, pp. 2451–2466, Jun. 2017.

[22] D. Zhou, M. Sheng, R. Liu, Y. Wang, and J. Li, "Channel-aware mission scheduling in broadband data relay satellite networks," *IEEE J. Sel. Areas Commun.*, vol. 36, no. 5, pp. 1052–1064, May 2018.

[23] M. Bisgaard, D. Gerhardt, H. Hermanns, J. Krčál, G. Nies, and M. Stenger, "Battery-aware scheduling in low orbit: The GomX–3 case," in *Formal Methods—FM*. Cham, Switzerland: Springer, 2016, pp. 559–576.

[24] G. Nies *et al.*, *Mastering Operational Limitations of LEO Satellites—The GOMX-3 Approach*, Int. Astronautical Federation, Paris, France, Sep. 2016, pp. 1–15.

[25] M. R. Jongerden and B. R. Haverkort, "Which battery model to use?" *IET Softw.*, vol. 3, no. 6, pp. 445–457, 2009.

[26] H. Hermanns, J. Krcál, and G. Nies, "How is your satellite doing? Battery kinetics with recharging and uncertainty," *Leibniz Trans. Embedded Syst.*, vol. 4, no. 1, pp. 1–28, 2017.

[27] N. Karmarkar, "A new polynomial-time algorithm for linear programming," *Combinatorica*, vol. 4, no. 4, pp. 373–395, Dec. 1984. [Online]. Available: https://doi.org/10.1007/BF02579150

[28] H. Marchand, A. Martin, R. Weismantel, and L. Wolsey, "Cutting planes in integer and mixed integer programming," *Discr. Appl. Math.*, vol. 123, nos. 1–3, pp. 397–446, 2002. [Online]. Available: http://www.sciencedirect.com/science/article/pii/S0166218X01003481

[29] *IBM ILOG CPLEX Optimization Studio*. Accessed: Nov. 2019. [Online]. Available: https://www.ibm.com/products/ilog-cplex-optimization-studio

[30] *Gurobi Optimizer*. Accessed: Nov. 2019. [Online]. Available: http://www.gurobi.com

[31] J. Clausen, *Branch and Bound Algorithms-Principles and Examples*, Dept. Comput. Sci., Univ. Copenhagen, Copenhagen, Denmark, Mar. 1999, pp. 1–30.

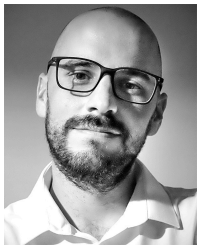

Juan A. Fraire is an Assistant Researcher with the National Research Council of Argentina and an Associate Professor with FAMAF, Universidad Nacional de Córdoba, Saarland University, Germany, and a Guest Professor with Politecnico di Torino, Italy. He has been the Founder and the Chair of the Annual Space-Terrestrial Internetworking Workshop since 2014. He has coauthored more than 45 papers published in international journals and leading conferences. His research focuses on spaceborne networking and applications.

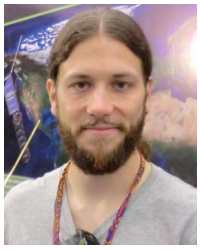

Gilles Nies is currently pursuing the Doctoral degree with the Group of Dependable Systems and Software, Saarland University, Germany. His research interests encompass the formal analysis and verification of complex systems in the broadest sense with a focus on formal energy storage models and specifically battery models in the context of e-mobility and nanosatellites.

Carsten Gerstacker is currently pursuing the master's degree with Saarland University, Germany. His research interest includes the verification and synthesis of reactive systems.

Holger Hermanns is a Full Professor with Saarland University, Saarbrücken, Germany, holding the Chair of Dependable Systems and Software on Saarland Informatics Campus, and a Distinguished Professor with the Institute of Intelligent Software, Guangzhou, China. He has authored or coauthored more than 200 peer-reviewed scientific papers. His research interests include modeling and verification of concurrent systems, resource-aware embedded systems, compositional performance and dependability evaluation, and their applications to energy informatics. He is a member of Academia Europaea, ERC Advanced Grantee, and spokesperson of the Center for Perspicuous Computing, TRR 248.

Kristian Bay is currently working as Senior Software Engineer with Beumer Group and holds more than 25 years experience in software development ranging from embedded systems to full-stack distributed systems. From 2015 to 2018, he was working with GomSpace as a Senior Software Engineer. From 2017 to 2018, he was involved in maintaining and developing ground station services for the GOMX-4 mission as well as coordinating the GOMX-4 activities during LEOP and during the main mission activities, including coordination and execution of platform and payload experiments.

Morten Bisgaard received the Ph.D. degree in autonomous systems from Aalborg University. He is currently the Head of the Spacecraft and Solution Department with GomSpace A/S and has more than 15 years experience from the new-space industry. He has authored or coauthored more than 30 papers in conferences and journals.